J. Synchrotron Rad. (1999). **6**, 532–534

Relationship between the electronic and local structure in $BaBi_{1-x}Pb_xO_3$ and $Ba_{1-x}K_xBiO_3$ perovskites

Alexander Ignatov

Departement of Quantum Electronics, Moscow Engineering Physics Institute, Kashirskoe sh. 31, 115409 Moscow, Russia and Deptartment of Physics, Southern Illinois University, Carbondale, IL 6290-4401, USA
E-mail: ignatov@physics.siu.edu

Starting from 2D Peierls-Emery Hamiltonian in the hole representation the relationship between the electronic and local structure in $BaBi_{1-x}Pb_xO_3$ and $Ba_{1-x}K_xBiO_3$ perovskites has been investigated. I attempt to provide some grounding in the model of charge disproportionation: $2Bi^{+4} \rightarrow Bi^{+3} + Bi^{+3}\underline{L}^2$. Calculated local structure of parent $BaBiO_3$ agrees reasonably well with those supplied by XAFS and XRD measurements. Both breathing and tilting distortions of the Bi-O bonds were found. Evolution of the local structure with hole(electron) doping was evaluated numerically and compared with EXAFS data. The low temperature anomalies in the local structure of $BaBiO_3$ are discussed.

Keywords: charge disproportionation, electronic structure, local structure, XAFS, perovskites

1. Introductions

The discovery of superconductivity at T_c~30K in $Ba_{1-x}K_xBiO_3$ (Mattheiss *et al.*, 1988) has generated renewed interest in $BaBi_{1-x}Pb_xO_3$ (T_c~12K). In spite of a large amount of the work dedicated to these perovskites not only the superconducting but also the normal electronic properties and local structure in the metallic phase are still not well understood. These problems seem to originate from the fact that the covalent materials have strong correlations between the electronic and lattice degrees of freedom. Therefore, it is important to carefully study both the electron-electron and electron-lattice interactions and their signature in various response functions.

2. Model

I have used a 2D Peierls-Emery Hamiltonian in the hole representation which includes all nearest-neighbor interactions:

$$H^{total} = H^{elect} + H^{lat} + H^{e-ph}$$

$$H^{elect} = \sum_{i,\sigma} \varepsilon_i n_{i,\sigma} + U_m \sum_i n_{i,\uparrow} n_{i,\downarrow} + \sum_{k,\sigma} \varepsilon_k n_{k,\sigma} + U_p \sum_k n_{k,\uparrow} n_{k,\downarrow} +$$

$$V_{mp}(u_k) \sum_{<i,k>\sigma,\sigma'} n_{i,\sigma} n_{k,\sigma'} + V_{pp}(|\mathbf{r}_k - \mathbf{r}_{k'}|) \sum_{<k\neq k'>\sigma,\sigma'} n_{k,\sigma} n_{k',\sigma'} -$$

$$T_{mp}(u_k) \sum_{<i\neq k>\sigma,\sigma'} (\hat{c}^+_{i,\sigma} \hat{p}_{k,\sigma'} + h.c) - T_{pp}(|\mathbf{r}_k - \mathbf{r}_{k'}|) \sum_{<k\neq k'>\sigma,\sigma'} (\hat{p}^+_{k,\sigma} \hat{p}_{k',\sigma'} + h.c)$$

$$H^{lat} = \sum_k \frac{1}{2M_k} p_k^2 + \sum_{k,k'} \frac{1}{2!} K_{k,k'} u_k u_{k'} + \sum_{k,k',m,m'} \frac{1}{4!} W_{k,k',m,m'} u_k u_{k'} u_m u_{m'}$$

$$H^{e-ph} = -\sum_i \lambda_i^{e-ph} \sum_{k,\sigma} n_k u_{k,\sigma}$$

Here, $\hat{c}^+_{i,\sigma}$ ($\hat{p}^+_{k,\sigma}$) creates a hole with spin σ at site $i(k)$ in the Bi 6*s* (O $2p_{\prime\prime}$) orbitals respectively; $n_{i,\sigma} = \hat{c}^+_{i,\sigma}\hat{c}_{i,\sigma}$ and $n_{k,\sigma} = \hat{p}^+_{k,\sigma}\hat{p}_{k,\sigma}$ are hole number operators; ε_i and ε_k are Bi 6*s* and O 2*p* energies; U_m and U_p are Bi and O on-site Coulomb repulsions; V_{mp} and V_{pp} are off-site Bi-O and O-O Coulomb repulsions.

Electron-lattice coupling is introduced through the Bi-O and O-O nearest-neighbor hoppings and Coulomb repulsions. These parameters are assumed to be modified by the local displacements, u_k of oxygen atoms depicted in Fig. 1*(a)*. They have the bond length dependences of $r_{Bi\text{-}O}^{-4}$ for T_{mp} and V_{mp} and $r_{O\text{-}O}^{-3}$ for T_{pp} and V_{pp}. Both the breathing and tilting displacements of oxygen atoms were involved.

For $BaBiO_3$ that corresponds to the undoped system, the number of holes, N= 4, (i.e. one hole per every Bi site) is assumed. Both electron- doped (N= 2,3) and hole- doped systems (N= 5,6) were investigated. The kinetic part of the lattice was neglected. The Hamiltonian was diagonalized using Lanczos algorithm. The Hamiltonian's parameters (in eV) used for calculations were:

$$\Delta = \varepsilon_k - \varepsilon_i = -4,\ U_m = 3,\ U_p = 1,\ V_{mp}^{(0)} = 1.5,\ V_{pp}^{(0)} = 0,$$

$$T_{mp}^{(0)} = 2,\ T_{pp}^{(0)} = 1,\ K_{\parallel} = 18 \text{ eV Å}^{-2},\ K_{\perp} = 0.075 \text{ eV Å}^{-2},$$

$$W_{\parallel} = 67.2 \text{ eV Å}^{-4},\ W_{\perp} = 19.5 \text{ eV Å}^{-4},\ \lambda_i^{e-ph} = 0.$$

The problem of the local structure refinement is formulated as follows: $E^{total}(\{u_k\}) \rightarrow min.$, in other words, one should find a set of oxygen atom displacements, $\{u_k\}$ which minimizes the total energy of the cluster. Energy minimum was achieved for the breathing displacements of $u_x^1 = u_y^2 = -u_x^3 = -u_y^4 = 0.106$Å and tilting displacements $u_y^1 = u_x^2 = -u_y^3 = -u_x^4 = 0.167$Å shown in Fig. 1. The calculated local structure of $BaBiO_3$ agrees reasonably well with those supplied by XAFS (Boyce *el al.*, 1992) and XRD (Pei *et al.*, 1990) measurements.

I have found that to add two holes on half of the $Bi\text{-}O_6$ complexes (Bi^{+3}+ $Bi^{+3}\underline{L}^2$) costs less energy than to put one hole on each of the $Bi\text{-}O_6$ complexes ($Bi^{+3}\underline{L}$+ $Bi^{+3}\underline{L}$). This provides some grounding in the model of charge disproportionation: $2Bi^{+4} \rightarrow Bi^{+3} + Bi^{+3}\underline{L}^2$ proposed earlier (Ignatov, 1995, 1998). Here $\underline{L}^2$ denotes two holes spread around four (six) oxygen atoms surrounding the Bi ion in 2D (3D) compounds.

The majority of charge density resides at the oxygen sites, while the charge density at Bi sites alternates between very small (at Bi(2) site) and small (at Bi(1) site). Around a Bi site with the larger charge density, four surrounding O atoms are displaced toward it symmetrically. They gain energy by increasing bond-charge density and thus enhancing covalency on the four Bi-O bonds around the central Bi site. The electron-electron interaction forms a $Bi^{+3}\underline{L}^2\text{-}O_4$ complex that consists of four stronger Bi-O bonds around a Bi(1) site. The on-site repulsion at Bi sites U_m is too weak to have magnetic moments there.

The ground state in $BaBiO_3$ may be regarded as a regular lattice of covalent molecules, where each molecule consists of two holes spread around four (for the 2D model considered here) or six (for real compounds) oxygen atoms surrounding the Bi ion. This covalent molecule can be viewed as a bipolaron since the two holes are self-trapped within the $Bi^{+3}\underline{L}^2\text{-}O_{4(6)}$ complex.

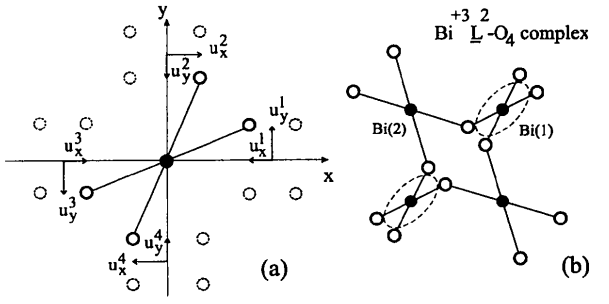

Figure 1
(a) Components of the oxygen atom displacement in the 2D model. Bi (O) atoms are indicated by closed (open) circles. Possible O atom displacements corresponding to energy minima are shown by dashed open circles. The O atoms move in essentially anharmonic, asymmetric four-well potentials (eighth-well potentials in real $BaBiO_3$). *(b)* Sketch of displacement configuration (orthorhombic distortions) that minimizes the total energy of the cluster. The $Bi^{+3}\underline{L}^2$-O_4 complex consists of four stronger Bi-O bonds around the Bi(1) site. Two holes are self-trapped within the complex.

3. Local structure of doped compounds

The oxygen atom displacement in the direction perpendicular to the Bi-O bond *vs* number of the holes in the cluster is shown in Fig. 2. There are two minima in doped compounds. For example, for N= 5, the minimum corresponding to the larger(smaller) distortions refers to the metal(insulator) state. Using the same set of the parameters of the Hamiltonian as for $BaBiO_3$ I found out that the minimum corresponding to the larger oxygen displacements is a global minimum. However, one should be very careful in interpreting the fact: the small increase in spring constants would results in replacing the global minimum with the local one. Thus, the calculations point out the possible (i) *increase in local structure distortions* and (ii) *phase separation* in doped compounds. To verify the theoretical predictions let me turn to the experimental XAFS data.

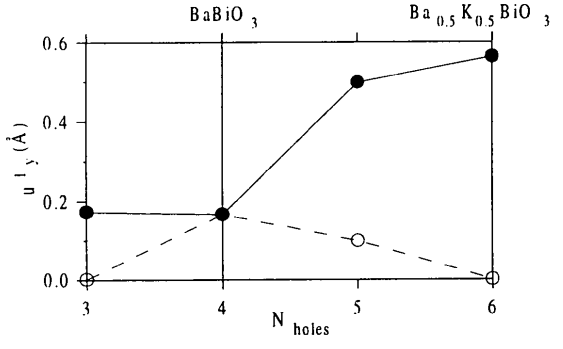

Figure 2
Calculated magnitude of tilting displacement *vs* hole(electron) doping. Closed(open) circles correspond to the global(local) local mimima.

The knowledge of the local structure around the Ba site is especially useful to study the oxygen atom displacements that are perpendicular to the Bi-O bond. The Ba L_3 edge XAFS measurements of the $BaBi_{1-x}Pb_xO_3$ (x=0,0.25,0.75) and $Ba_{0.6}K_{0.4}BiO_3$ were performed on the beamline EXAFS-II of HASYLAB at DESY in the temperature range of 30-300K. We have found that two groups of Bi-O distances may be extracted for extracted for all compounds (Ignatov *et al.*, 1995). For example, for the oxygen shell of $Ba_{0.6}K_{0.4}BiO_3$ at room temperature we find: R_1= 2.59±0.03Å, N_1= 2±1; and R_2= 3.16±0.03Å, N_2= 10±1 for the first and second groups, respectively. Moreover, the K doping gives rise to separation of the Ba-O distances from Δr= 0.42 Å in $BaBiO_3$ to Δr= 0.57 Å in $Ba_{0.6}K_{0.4}BiO_3$. This situation may be best shown using a pair distribution function (PDF). The PDFs of Ba-O atoms in $BaBi_{1-x}Pb_xO_3$ (x=0,0.75,1) and $Ba_{0.6}K_{0.4}BiO_3$ at T= 35 K are depicted in Fig. 3. They were generated from the Fourier-filtering contribution of the Ba-O bonds in the range of k= 2-7.6 $Å^{-1}$, using EDARDF code (Kuzmin, 1996).

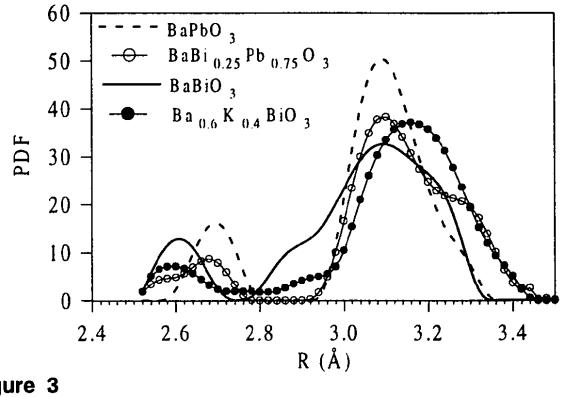

Figure 3
Pair distribution functions of Ba-O atoms in $BaBi_{1-x}Pb_xO_3$ (x=0,0.75,1) and $Ba_{0.6}K_{0.4}BiO_3$ perovskites, T= 35 K.

This result contradicts the simple cubic structure deduced from the diffraction experiment (Pei *et al.*, 1990). The results of XAFS study of $Ba_{0.6}K_{0.4}BiO_3$ (Yacoby *et al.*, 1997) pointed out two set of Ba-O distances as well. However, simple estimations give the decrease of Ba-O distance separation in $Ba_{1-x}K_xBiO_3$ as x rises from 0 to 0.4, that disagrees with the present results.
The Bi L_3 XAFS measurements were performed on the beamline A1 of HASYLAB at DESY. The Fourier-filtered contribution from the Bi-O bonds of $Ba_{0.6}K_{0.4}BiO_3$ at T= 5 K is shown in Fig. 4. It was fitted in terms of two models: one or two different Bi-O distances were assumed. The local structure parameters for the 1S and 2S models were derived from the non-linear least-squares fits over the range of k= 3-16 $Å^{-1}$, using the curved wave EXAFS theory. The quality-of-fit parameter for the 2S model is 1.6 times smaller than that for 1S mode. Therefore, *two different Bi-O distances* may be extracted in $Ba_{0.6}K_{0.4}BiO_3$ at 5 K: R_1 = 2.10±0.02 Å and R_2 = 2.22±0.02 Å. These distances were observed with the equal coordination number N_1=N_2= 3.

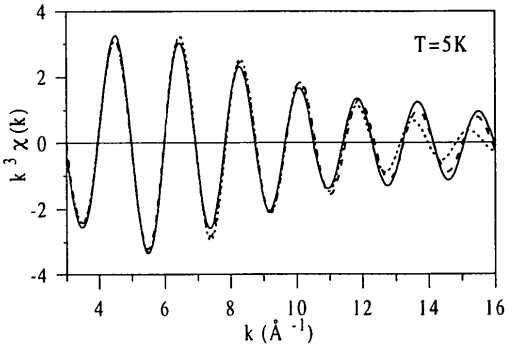

Figure 4
Comparison ot the Fourier-filtered contribution from the Bi-O bonds in $Ba_{0.6}K_{0.4}BiO_3$ (solid line) with fitting curves corresponding to the 1S (dots) and 2S (dashed line) models. The Fourier-transform range is 2.1-17.6 $Å^{-1}$, square window; the backtransform range is r= 1-2 Å.

To summarize, the combined analyses of the Ba L_3 and Bi L_3 edges XAFS provide clear evidence for existence of marked local structure distortions in metallic $Ba_{0.6}K_{0.4}BiO_3$. Though the Bi-O peak separation decreases with K doping it *does not disappear* at x= 0.4, in contract to earlier XAFS studies (Heald, *et al.*, 1989; Salem-Sugui, *et al.*, 1991).

To characterize the order of distortions in $Ba_{1-x}K_xBiO_3$ an angle of deviation of the O atoms from linear Bi-O-Bi chains, α has been employed. The larger the distortions the larger the angle is. Taking into account Bi-Bi separation of 4.27 Å one can readily evaluate α= 11±2 ° for $Ba_{0.6}K_{0.4}BiO_3$. Similar estimation for pure $BaBiO_3$ based on XAFS data (Boyce *et al.*, 1990) gives $\alpha \sim 9$ °. Therefore, the metal-to-insulator phase transition in $Ba_{1-x}K_xBiO_3$ is accompanied with *the increase of local lattice distortions rather than their decrease*, as it was expected earlier. The experimental XAFS results support the theoretical predictions of the local structure instability in $BaBi_{1-x}Pb_xO_3$ and $Ba_{1-x}K_xBiO_3$ perovskites.

4. The low temperature anomalies

The earlier XAFS studies of $BaBiO_3$ and superconducting $BaBi_{0.25}Pb_{0.75}O_3$ (Boyce *el al.*, 1990) did not show any structural transformation between 4 and 300 K. However, we have found that the Bi-O distances in $BaBi_{1-x}Pb_xO_3$ (x=0,0.25) (Menushenkov *et al.*, 1997) as well as the Ba-O distances in $BaBi_{1-x}Pb_xO_3$ (x=0,0.25,0.75) and $Ba_{0.6}K_{0.4}BiO_3$ (Ignatov *et al.*, 1995) increase with decreasing temperature. The Debye-Waller factors evaluated from two- sphere fitting show a deviation from the standard temperature dependence with anomalous increase below 60-90 K.

To give qualitative description of the low temperature anomalies in the local structure of these perovskites I have considered a pure $BaBiO_3$ and only one phonon mode when the oxygen atoms move perpendicular to the Bi-O bond directions. I assume the electron-phonon coupling constant to be a function of the temperature (Hardy & Flocken, 1988), so far as the oxygen atoms move in essentially anharmonic potentials. The temperature dependence of the other parameters of the Hamiltonian are neglected. The local structure of $BaBiO_3$ was calculated for the two cases: for λ_i^{e-ph}=0.05 and λ_i^{e-ph}=0.1, that corresponds qualitatively to the transition from high to low temperature. For λ_i^{e-ph}=0.05 the components of oxygen atom displacements are very similar to that discussed in Sect. 2. However, for λ_i^{e-ph}=0.1 the picture becomes much more complicated: every local minimum shown in Fig. 1*(a)* is replaced by two asymmetric local minima separated by ~0.1 Å. It should be note that such a replacement appears at rather small partial value of λ_i^{e-ph} that is in agreement with a small total value of λ^{e-ph}~0.7-0.9 (Batlogg *et al.*, 1988). The generation of the two local minima instead of one minimum results in broadening or even apperance of the multipeak structure of the PDF. This is exactly what is seen in the Bi L_3 XAFS data in Fig. 5.

Thus, the electron-phonon interaction along with the non-linear electron-electron interactions might be responsible for the low temperature anomalies in the local strucrute of $BaBi_{1-x}Pb_xO_3$ and $Ba_{1-x}K_xBiO_3$ perovskites.

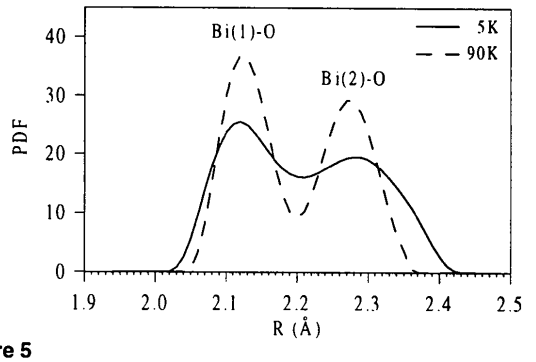

Figure 5
Pair distribution functions of Bi-O atoms *vs* temperature in $BaBiO_3$.

5. Conclusions

The relation of electronic and local structures in $BaBi_{1-x}Pb_xO_3$ and $Ba_{1-x}K_xBiO_3$ perovskites has been investigated in frame of the 2D Peierls-Emery Hamiltonian. This approach allows one to provide many-body basis for $2Bi^{+4} \rightarrow Bi^{+3} + Bi^{+3}\underline{L}^2$ description of the charge disproportionation to evaluate the local structure of the Bi-O bonds *vs* the hole(electron) doping, and to give at least qualitative description of the low temperature anomalies in the local structure of these compounds. These results indicate the need to consider both non-linear electron-electron and electron-phonon interactions to obtain satisfactory description for electronic and local structure of real perovskites.

I would like to thank K. Attenkofer, V.A. Chernov, J. Feldhaus, A.A. Ivanov, K.V. Klementev, A.P. Menushenkov, A.A. Meshkov, A.P. Rusakov, and M. Tischer who have also been involved at the different stages of this work. I wish to thank the HASYLAB and VEPP-3 Program Committees for their approval of the research projects.

References

Batlogg, B., Cava, R.J., Rupp, L.W.Jr, Mujsce, A.M., Krajewski, J.J., Remeika, J.P., Peck, W.F.Jr, Cooper, A.S. & Espinosa, G.P. (1988). *Phys. Rev. Lett.* **61**, 1670-1673.

Boyce, J.B., Bridges, F.G., Claeson, T., Geballe T.H. & Remeika, J.M. (1990). *Phys. Rev.* **B41**, 6306-6314.

Boyce, J.B., Bridges, F.G. & Claeson, T. (1992). *Physica Scripta* **42**, 71-75. See also referenses therein.

Hardy, J.R. & Flocken, J.W. (1988). *Phys.Rev. Lett.* **60**, 2191-2194.

Heald, S.M., DiMarzio, D., Croft, M., Hegde, M.S., Li, S. & Freenblatt, M. (1989). *Phys. Rev.* **B40**, 8828-8833.

Ignatov, A.Yu. (1995). *Ph.D. thesis, Moscow Engineering Physics Institute*, 1-200. (in Russian).

Ignatov, A.Yu., Menushenkov, A.P., Feldhaus, J. & Klementev, K.V. (1995). *HASYLAB Annual Report 1995*, II-316.

Ignatov, A.Yu. (1998). *Nucl. Instrum. Methods*, **A405**, 359-364.

Kuzmin, A. (1995). *Physica* **B208&209**, 175-176.

Mattheiss, L.F., Gyogry, E.M. & Jonson, D.W. Jr. (1988). *Phys. Rev.* **B37**, 3745-3746.

Menushenkov, A.P., Benazeth, S., Purans, J., Ignatov, A.Yu. & Klementev, K.V. (1997). *Physica* **C277**, 257-264.

Pei, S., Jorgensen, J.D., Dabrowski, B., Hinks, D.G., Richards, D.R., Mitchell, A.W., Newsam, J.M., Sinha, S.K., Vaknin, D. & Jacobson, A.J. (1990). *Phys. Rev.* **B41**, 4126-4141.

Salem-Sugui, S.Jr, Alp, E.E., Mini, S.M., Ramanathan, M., Campuzano, J.C., Jennings, G., Faiz, M., Pei, S., Dabrovski, B., Zheng, Y., Richards, D.R. & Hinks, D.G. (1991). *Phys. Rev.* **B43**, 5511-5115.

Yacoby, Y., Heald, S.M. & Stern, E.A. (1997). *Solid State Commun.* **v101**, 801-806.

(Received 10 August 1998; accepted 1 December 1998)